

A Simple and Provable Approach for Learning on Noisy Labeled Multi-modal Medical Images

Anonymous Authors

ABSTRACT

Deep learning for medical image classification needs large amounts of carefully labeled data with the aid of domain experts. However, data labeling is vulnerable to noises, which may degrade the accuracy of classifiers. Given the cost of medical data collection and annotation, it is highly desirable for methods that can effectively utilize noisy labeled data. In addition, efficiency and universality are essential for noisy label training, which requires further research. To address the lack of high-quality labeled medical data and meet algorithm efficiency requirements for clinical application, we propose a simple yet effective approach for multi-field medical images to utilize noisy data, named **Pseudo-T correction**. Specifically, we design a noisy label filter to divide the training data into clean and noisy samples. Then, we estimate a transition matrix that corrects model predictions based on the partitions of clean and noisy data samples. However, if the model overfits noisy data, it makes noisy samples more difficult to detect in the filtering step, resulting in inaccurate transition matrix estimation. Therefore, we employ gradient disparity as an effective criterion to decide whether or not to refine the transition matrix in the model's further training steps. The novel design enables us to build more accurate machine-learning models by leveraging noisy labels. We demonstrate that our method outperforms the state-of-the-art methods on three public medical datasets (dermoscopic images, histopathology slide images, X-Ray) and achieves superior computational efficiency over the alternatives.

CCS CONCEPTS

• Computing methodologies → Machine learning.

KEYWORDS

Noisy Label Learning, Multi-field Data, Medical Image Analysis, Pseudo-label

1 INTRODUCTION

Medical image classification plays a vital role in clinical treatment tasks and diagnosis applications [29, 37, 38]. The success of these classification tasks is contingent upon learning highly discriminative representations using deep neural networks from a huge amount of carefully labeled data with the assistance of domain experts. However, labeling samples by medical experts for medical

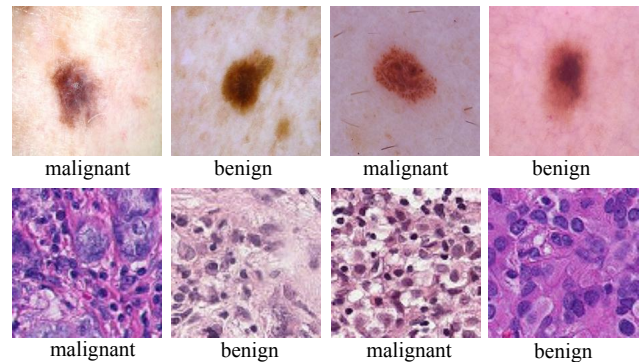


Figure 1: Examples of typical confusing malignant and benign images from skin lesions and histology lymph nodes, which are prone to inaccurate labeling during the practical annotation process.

image classification is expensive, and collecting labels may suffer from the noises [17]. For instance, as demonstrated in Fig. 1, the malignant histology lymph node images exhibit colors and structures that are strikingly similar to benign ones. This indicates that noisy annotations are an unavoidable part of medical image processing in real-world settings.

With the development of deep learning, various methods have been widely used in medical image classification [3, 6, 28] to solve the issue of noisy labeling. There exist two general resolving directions, one is to collect more data [7, 34], although data collection methods are typically affected by noisy labels. Another way is to fully utilize clean labels while ignoring the noisy labels [11, 12, 18, 35]. Despite making better annotations, these methods are over-complex in the architecture design compared with vanilla classification training, thus becoming sensitive to outliers. Equally, simply and provably processing noisy labeled medical data is significant to assist doctors in diagnosis, few researches have been conducted in medical image classification. Specifically, the existing state-of-the-art method RMIC [37] introduces a complicated teacher-student model that has two carefully designed distillation modules. This is problematic as it costs more resources and time to yield a model. Improving model efficiency is equally important as maintaining model accuracy. Apparently, many clinical applications require real-time decision [23] to allow human-in-the-loop, while a complex model cannot meet such a requirement. Besides, sophisticated deep learning models for healthcare are challenging to install and update on power-constrained devices [21]. Additionally, it is critical to employ simple noisy label training, while the correctness is provable. Such methods have merely been studied so far in medical image classification.

Despite their extraordinary effectiveness, it has been repeatedly observed that the performance of these methods is easily influenced

Permission to make digital or hard copies of all or part of this work for personal or

Unpublished working draft. Not for distribution. This work is derived from a preprint and is not intended for publication. It is distributed for profit or commercial advantage and that copies bear this notice and the full citation on the first page. Copyrights for components of this work owned by others than the author(s) must be honored. Abstracting with credit is permitted. To copy otherwise, or republish, to post on servers or to redistribute to lists, requires prior specific permission and/or a fee. Request permissions from permissions@acm.org.

ACM MM, 2024, Melbourne, Australia

© 2024 Copyright held by the owner/author(s). Publication rights licensed to ACM.

ACM ISBN 978-x-xxxx-xxxx-x/YY/MM

<https://doi.org/10.1145/nnnnnnnn.nnnnnnnn>

by the bias of the training set in complex real-world scenarios [37]. For instance, such bias could come from the variations of disease patterns. A typical issue is that these data biases can cause noise labeling problems. Therefore, an important topic in the realm of medical image analysis is handling multimodal noise. As far as we know, recent research has used cross-modal weak supervision by utilizing convolutional neural networks (CNN). While various previous cross-modal weak supervision methods have shown promise in medical applications, the research conducted to date has been on generating weak labels in an application-specific manner [5]. There is no theoretical analysis that describes the performance expectations of the resulting models, which would support any of these application-specific cross-modal weak supervision approaches. Additionally, these methods can only handle MRI or CT, and the generalizability needs to be improved.

By analyzing the existing noisy label learning work for medical image classification, we find that most of the existing methods focus on detecting and utilizing single-mode clean labels only. Nevertheless, these methods are heuristic without provable properties and require much more training parameters than vanilla classification model [18, 21, 23]. Noticing the gaps, we contribute as follows:

- We propose a simple and provable noisy label learning strategy that can leverage the labels of clean and noisy data. Specifically, we estimate a transition matrix to correct model outputs to fit the observed labels. The resulting method is called **Pseudo-T correction**.
- We theoretically prove that **Pseudo-T correction** achieves the same optimal as learning with all clean labels on expectation. To overcome the model overfitting noisy data, we employ gradient disparity as a criterion so that the fixed transition matrix can be accurately modeled by exploiting the noise.
- We proved **Pseudo-T correction** is easier to implement by comparing our method with the state-of-the-art methods. While achieving comparable results, our method utilizes a simpler model and presents theoretical guarantees. Our method also has been extensively validated on three medical image noisy labels with public datasets. The proposed approach outperforms previous learning from noisy labeled data methods and steadily increases prediction accuracy across various datasets.

2 RELATED WORK

In this section, we focus on the previous works on noisy labels with deep neural networks and sample clustering, which builds the foundation for the approach we propose.

2.1 Deep Learning With Noisy Labels

To mitigate the impacts of noisy labels on deep learning, researchers proposed approaches to increase the deep neural networks' robustness in recent years.

Attempts have been made to evaluate the training labels' correctness. The concept of a supervisor model, MentorNet, is introduced by Jiang et al. [11]. MentorNet is initialized to approximate a pre-defined sample weighting scheme. During training, it learns with the base deep learning network and re-weights the sample labels

based on their reliability. However, the ubiquity of ambiguous hard samples makes the method difficult for medical images, since the images of two classes can be pretty similar. Other than that, other approaches tend to gradually correct the target labels according to the model's prediction. Reed et al. [27] proposed the bootstrapping method, considering the training label confidence by evaluating the model prediction consistency on similar input data. Instead of trusting all training labels to be ground truth, the model's current prediction also plays an important role in deciding the model's label targets. Based on the bootstrapping approach, Iscen et al. [10] penalizes prediction divergence between samples with similar features via an additional consistency loss layer. However, this method introduces additional computational costs to determine the similarity and weighted predictions. It is usually costly for medical image datasets, which are usually large in image feature dimensions. Other than that, the samples with noisy labels are not utilized.

Meanwhile, some methods increase the training loss robustness to noisy labels. Sukhbaatar et al. [30] allows the model to capture the label transition matrix by introducing a constrained linear noise layer, handling both label flips and outliers. Patrini et al. [25] proposed two loss correction procedures, which are independent of the neural network's application and architecture. With an assumption of possessing a known label transition matrix T , the loss can be corrected by multiplying with the inverse of T . However, these methods require a certain amount of clean data ahead of time, and the transition matrix is hard to capture due to the complexity of medical image data. Being independent of any prior information, [13] filters noisy labels and trains on the labels with high confidence by selectively applying negative and positive learning.

2.2 Noisy Labels in Medical Imaging

Labeling medical images is expensive and time-consuming as it requires human experts to manually classify them. The data source can also inevitably suffer from noises [17]. Some ambiguous images may confuse experts and some large-scale datasets require automation tools to extract labels, resulting in a certain level of wrong annotation [37]. To address such an issue, many researches were conducted.

Some researchers focus on identifying noisy data from clean datasets. Dgani et al. [4] trains a stochastic matrix to determine the likelihood that a label is noisy. Zhu et al. [39] proposes a label quality evaluation criteria to only feed preferable data to optimize the network's parameters. Kim et al. [12] developed the FINE framework to filter out noisy data based on their eigenvectors.

Rather than implementing a noisy data filter, some approaches also consider utilizing them to enhance feature detection, and meanwhile, suppressing their influence by re-weighting. Xue et al. [36] designs an iterative learning framework to identify wrongly annotated data and hard samples. A module is also developed to consider the usefulness of those data by assigning appropriate weights. Xue et al. [37] introduces the RMIC method, which involves a co-training framework. The framework includes two student-teacher models, which classify clean and noisy labels independently. Their classifications are fed to one another as new inputs in the next training cycle. Within a student-teacher network, the clean and noisy data are respectively considered by four losses. To increase the teacher

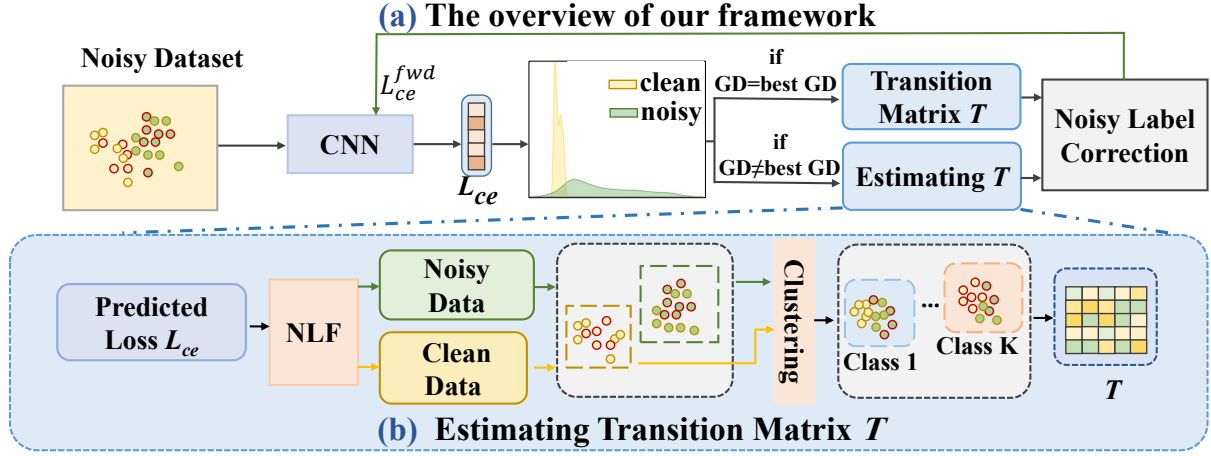


Figure 2: The proposed Pseudo-T correction method, including (a) the overview of our framework, (b) indicates the specific procedure of estimating the transition matrix. We first input the noisy dataset into our network and divide all samples into noisy and clean groups. To tackle the challenge of noisy label detection, a noisy label filter (NLF) divides all the training data by leveraging the predicted cross-entropy loss of our network. Then, we design a transition matrix that corrects model predictions based on the partitions of clean and noisy data samples. To prevent overfitting of the model to noisy data, we utilize gradient disparity (GD) as a stopping criterion to determine whether to fix the transition matrix T in further model training steps.

network's robustness to noisy labels, its weight is updated by the student network's exponential moving average. The noisy labels are also utilized by a self-supervising learning strategy to improve the network's feature learning. Liu et al. [18] addresses the "noisy supervised domain adaptation" problem for medical imaging segmentation with S-CUDA, which also contains two peer networks. The high-confident noisy labels are identified and corrected by the network's predictions for future reuse.

2.3 K-Mean Clustering

K-mean clustering is one of the most widely used data mining algorithms, grouping up samples with the closest mean. In recent years, many efforts have been made to improve the K-mean algorithm efficiency. Leng et al. [15] chooses cluster initial points by comparing the data point distances with a small threshold. It refines the clusters and decides whether to merge them with an influence factor to measure the similarities between the two clusters. Napoleon and Lakshmi [22] proposes a more efficient K-mean clustering approach of two phases. The clustering centroids are initialized in the first phase, and data points are assigned and clusters are finalized in the second phase. Rauf et al. [26] further improves the clustering efficiency by first classifying data into K arrays of the same size. The clusters are then finalized in the second phase by computing and comparing the distance between data points to the cluster means.

3 PRELIMINARY

3.1 Problem Setting

We denote $\mathbf{x} \in \mathcal{X}$ as an image sample, $\tilde{\mathbf{y}} \in \{\mathbf{e}^i | i \in [K]\}$ is its observed label but possibly noisy (i.e., incorrect), a.k.a corrupted label. Here, K is the number of classes, \mathbf{e}^i is a K -dimensional one-hot vector, whose i -th entry is 1 and else are 0s. The ground truth

label $\mathbf{y} \in \mathcal{Y}$ of the sample is unknown. Under these setting, we train a classifier f_θ to fit the input images \mathcal{X} to their noisy labels $\tilde{\mathcal{Y}}$, we aim to optimize the our classifier f_θ with $\{\mathcal{X}, \tilde{\mathcal{Y}}\}$. The expected risk is defined as

$$\mathcal{R}(f_\theta) = \mathbb{E}_{(\mathbf{x}, \mathbf{y}) \sim P_{\mathcal{X}, \mathcal{Y}}} [\mathcal{L}(f_\theta(\mathbf{x}), \tilde{\mathbf{y}})], \quad (1)$$

where \mathcal{L} is cross-entropy loss, and we aim to find $\theta^* := \arg \min \mathcal{R}(f_\theta)$.

Label Noise. The process of label corruption can be represented by randomly flipping a true label \mathbf{y} to $\tilde{\mathbf{y}}$ with probability $p(\tilde{\mathbf{y}}|\mathbf{y})$. Thus, we observe samples from distribution $p(\mathbf{x}, \mathbf{y})$, where $p(\mathbf{x}, \mathbf{y}) = \sum_{\tilde{\mathbf{y}}} p(\tilde{\mathbf{y}}|\mathbf{y})p(\mathbf{y}|\mathbf{x})p(\mathbf{x})$. Such a transition can be expressed as a Markov transition matrix $T \in [0, 1]^{K \times K}$, with $T_{ij} := p(\tilde{\mathbf{y}} = \mathbf{e}^j | \mathbf{y} = \mathbf{e}^i)$, such that $p_{\tilde{\mathbf{y}}|\mathbf{x}} = T^\top p_{\mathbf{y}|\mathbf{x}}$.

3.2 Forward Correction in Learning on Label Noise

Risk correction is a simple yet effective approach in learning on label noise [25, 30, 31], among which forward correction dominates the performance in practice [25]. Without risk correction, training a neural network results in a prediction for the corrupted labels $\hat{p}(\tilde{\mathbf{y}}|\mathbf{x})$. Forward correction corrects the model prediction using transition matrix T . For classification based on minimizing cross-entropy, we have the forward corrected loss:

$$\mathcal{L}_{ce}^{fwd}(\mathbf{e}^i, \hat{p}(\mathbf{y}|\mathbf{x})) = -\log \hat{p}(\tilde{\mathbf{y}} = \mathbf{e}^i | \mathbf{x}) \quad (2)$$

$$= -\log \sum_{j=1}^K p(\tilde{\mathbf{y}} = \mathbf{e}^i | \mathbf{y} = \mathbf{e}^j) \hat{p}(\mathbf{y} = \mathbf{e}^j | \mathbf{x}) \quad (3)$$

$$= -\log \sum_{j=1}^K T_{ij} \hat{p}(\mathbf{y} = \mathbf{e}^j | \mathbf{x}). \quad (4)$$

Obviously, forward correction simply replaces the prediction trained on the noisy label $\hat{p}(\mathbf{y} = \mathbf{e}^j | \mathbf{x})$ with $T_{ij}\hat{p}(\mathbf{y} = \mathbf{e}^j | \mathbf{x})$.

Optimal in Forward Correction. In our context, the model is optimal in the sense that the minimizer of the corrected loss task coincides with the minimizer of the supervised task on true labels as if the perfect true labels \mathbf{y} can be observed.

THEOREM 3.1. (Equal optimal [25])

Given the forward corrected loss defined in Eq. 4 and T is non-singular, the minimizer of the corrected loss under the noisy label distribution is the same as the minimizer of the original loss under the true label distribution:

$$\begin{aligned} & \arg \min_f \mathbb{E}_{p(\mathbf{x}, \tilde{\mathbf{y}})} [\mathcal{L}_{ce}^{\text{fwd}}(Tf(\mathbf{x}), \tilde{\mathbf{y}})] \\ &= \arg \min_f \mathbb{E}_{p(\mathbf{x}, \mathbf{y})} [\mathcal{L}_{ce}(f(\mathbf{x}), \mathbf{y})] \end{aligned} \quad (5)$$

PROOF. Consider a link function $\psi : \Delta^{K-1} \mapsto \mathbb{R}^c$, which is invertible, the softmax function is the inverse link function in cross-entropy loss $\mathcal{L}_{ce} = -\log p(\mathbf{y} = \mathbf{e}^i) = -\log \frac{\exp(W_i^{(n)} \mathbf{x}^{(n-1)} + b_i^{(n)})}{\sum_{k=1}^c \exp(W_k^{(n)} \mathbf{x}^{(n-1)} + b_k^{(n)})}$, where n is the index of layers. Let $\mathbf{h}(\cdot)$ represent the features that pass through the softmax function. With proper composite loss properties of cross-entropy, the minimizer satisfies

$$\mathbf{h}^* = \arg \min_{\mathbf{h}} \mathbb{E}_{\mathbf{x}, \mathbf{y}} \mathcal{L}_{\psi}(\mathbf{y}, \mathbf{h}(\mathbf{x})) = \psi(p(\mathbf{y} | \mathbf{x})), \quad (6)$$

The proof follows [25]. Notice that:

$$\mathcal{L}_{ce}^{\text{fwd}}(\mathbf{y} = \mathbf{e}^i | \mathbf{x}) \quad (7)$$

$$= \mathcal{L}_{ce}(\mathbf{y}, T\psi^{-1}(\mathbf{h}(\mathbf{x}))) \quad (8)$$

$$= \mathcal{L}_{ce}^{\phi}(\mathbf{y}, \mathbf{h}(\mathbf{x})), \quad (9)$$

where $\phi^{-1} = \psi^{-1} \circ T$ and $\phi = (T^{-1}) \circ \psi$. Eq. 9 is the proper composite with link ϕ . Finally, from Eq. 9, the loss minimizer is

$$\begin{aligned} \mathbf{h}^* &= \arg \min_{\mathbf{h}} \mathbb{E}_{\mathbf{x}, \tilde{\mathbf{y}}} \mathcal{L}_{\phi}(\mathbf{y}, \mathbf{h}(\mathbf{x})) \\ &= \phi(p(\tilde{\mathbf{y}} | \mathbf{x})) \\ &= \psi(T^{-1}p(\tilde{\mathbf{y}} | \mathbf{x})) \\ &= \psi(p(\mathbf{y} | \mathbf{x})) \end{aligned}$$

□

4 EQUATIONS

4.1 Overview of the Framework

The goal of our work is to design a simple method for medical image analysis (see Fig. 2), while its correctness is provable. The overall training pipeline of our method is still described in Algorithm 1, Motivated by the essential theoretical guarantee in Theorem 3.1, we focus on applying the simple loss forward correction to medical tasks. However, the existing related works [25] typically assume the transition matrix T is known, which is impractical in medical applications. Medical image annotation contains complex human decisions, thus the real T is difficult to model. To estimate transition matrix T for forwarding correction, we first use label prediction by noisy label filter (NLF) (see Section 4.2.1) to distinguish clean

Algorithm 1 The training process of Pseudo-T correction.

Input: Training data $(\mathbf{x}, \mathbf{y}) \in (\mathcal{X}, \mathcal{Y})$, network $\mathbf{g}(\mathbf{x}; \theta)$, transition Matrix T , Epoch \mathcal{T} .

- 1: **repeat**
- 2: **for** $t \leftarrow 1$ to \mathcal{T} **do**
- 3: Batch \leftarrow Sample \mathbf{x}
- 4: Update \mathbf{g} by minimizing Eq. 4
- 5: Compute the cross-entropy loss \mathcal{L}
- 6: **if** GD \neq best GD
- 7: Clean & Noisy Sample $\mathbf{x} \leftarrow$ NLF (Sec. 4.2.1)
- 8: update transition Matrix T
- 9: **do**
- 10: $T_{ij} = p(\tilde{\mathbf{y}} = \mathbf{e}^j | \mathbf{y} = \mathbf{e}^i)$
- 11: **else**
- 12: fix transition Matrix T
- 13: Update label probabilistic modeling (Sec. 4.3)
- 14: **until** Convergence or \mathcal{T} reach maximum iterations.

samples from noisy samples that serve as the input for training the network. Then, the gradient disparity is applied as a stopping criterion to determine if the matrix is fixed. Finally, the transition matrix is applied to give different confidences to the clean and noisy labels, adapted to the noisy (see Section 4.2).

4.2 Estimating Transition Matrix T

The main purpose of this work is to estimate the transition matrix T for forward correction described in Section 3.2. To this end, the key step is to estimate the probability of a sample in class i is labeled as j , $T_{ij} = p(\tilde{\mathbf{y}} = \mathbf{e}^j | \mathbf{y} = \mathbf{e}^i)$. We propose to estimate the T_{ij} from the sample distribution of the training dataset. Given that corrupted labels $\tilde{\mathbf{y}} \in \tilde{\mathcal{Y}}$ are observed for N training samples if their corresponding true labels were known, we can count the number of samples N_i in class i . Hereby, the estimated transition matrix is expressed as $T_{ij} = p(\tilde{\mathbf{y}} = \mathbf{e}^j | \mathbf{y} = \mathbf{e}^i) \simeq \frac{|\{\tilde{\mathbf{y}}_n = \mathbf{e}^j | n \in [N_i]\}|}{N_i}$ for $i, j \in K$, where K is the number of classes.

4.2.1 Label Prediction by Noisy Label Filter (NLF). Patrini [25] assumes that the transition matrix T is known ahead of time. However, it is very hard to estimate such a matrix due to the complexity of medical images. To estimate transition matrix T , we first filter out clean data, which are believed to be correctly labeled in the dataset. Inspired by Xue et al. [37], we use an NLF to separate clean and noisy labels (a.k.a. wrong labels) based on data point-wise classification loss. More specifically, we compute the cross-entropy loss $\mathcal{L}(\hat{\mathcal{Y}}, \tilde{\mathcal{Y}})$ at the end of every epoch, where $\hat{\mathcal{Y}}$ is the prediction result/are the prediction results from $f_{\theta}(\mathcal{X})$. In our experiments, we use the cross-entropy loss as \mathcal{L} . Next, we input the loss into a noisy label filter (NLF) to predict $\{\mathcal{X}, \tilde{\mathcal{Y}}\}$ into clear $\{\mathcal{X}_c, \tilde{\mathcal{Y}}_c\}$ and noisy $\{\mathcal{X}_n, \tilde{\mathcal{Y}}_n\}$ samples. In detail, the NLF employs a two-component Gaussian Mixture Model (GMM) to cluster the samples into two groups based on their point-wise cross-entropy losses (i.e., $\ell_i = \hat{p}(\tilde{\mathbf{y}}_n | \mathbf{x}_n)$) for data point n .

The NLF method only selects the most confident samples as clean samples at the initializing stage, and the confidence threshold gradually decreases as the model becomes more robust. With a high

confidence threshold at the beginning, the consistency of the transition matrix T is maintained to the greatest extent. Meanwhile, we added gradient disparity (GD) as a stopping criterion to determine whether or not we should stop updating the transition matrix T .

4.2.2 Estimate N_i Via Clustering. The key challenge exposed is the true label being unknown, thus the number of samples N_i within a given true label i are unavailable. To tackle this issue, we propose an unsupervised pseudo-labeling strategy to estimate N_i . Specifically, we warm up the model without correction for τ steps and then perform clustering on the data feature representations to form K clusters, then assign each cluster a label based on the majority voting on a subset of clean samples within each cluster.

We first extract informative low-dimensional representations from the input medical images. Convolution neural networks (CNNs) show their efficiency in extracting the feature. Further, a recent work [16] shows that extracted features are representative and robust even when being trained on label noise. In our method, we use a ResNet-18 [9] as the feature extractor and one linear layer as the classifier training on the observed noisy labels. Then, we perform K-means clustering [26] on the extracted features to split the training data into K clusters.

4.2.3 Assign Pseudo Labels to Clusters. Towards estimating N_i , one step further is to assign a pseudo label to each cluster. For each cluster C_i , $0 \leq i < K$, we split the data samples $(\mathcal{X}^{C_i}, \mathcal{Y}^{C_i})$ in cluster C_i into clean $(\mathcal{X}_c^{C_i}, \mathcal{Y}_c^{C_i})$ (correctly labeled) and noisy $(\mathcal{X}_n^{C_i}, \mathcal{Y}_n^{C_i})$ (wrongly labeled) samples using the NLF method given in Section 4.2.1.

The label of each cluster depends on the majority voting on the prediction of clean data. To achieve more reliable pseudo labeling, we only choose the top 60% of the clean data given the noise level in medical data annotation is typically small high (*i.e.*, $\leq 40\%$) for mapping each C_i to a non-overlapped pseudo-class.

4.2.4 Estimate T_{ij} via Counting. After labeling each cluster, we denote the number of each class $j \in [K]$ in cluster C_i with pseudo true label i as $c_i^j = |\{\tilde{\mathbf{y}}_n = j | n \in |C_i|\}|$ and $\sum_{j=1}^K c_i^j = |\mathcal{Y}_c^{C_i}|$. Thus, c_i^j is achieved by counting the number of samples in each class based on the corrupted labels $\tilde{\mathbf{y}} \in \tilde{\mathcal{Y}}$. For $i, j \in K$, we have the estimation of transition matrix T written as

$$T_{ij} = p(\tilde{\mathbf{y}} = \mathbf{e}^j | \mathbf{y} = \mathbf{e}^i) \simeq \frac{|\{\tilde{\mathbf{y}}_n = j | n \in [N_i]\}|}{N_i} \simeq \frac{c_i^j}{|C_i|}. \quad (10)$$

For Estimate T_{ij} , the model will learn the clean data in the early epochs based on the memorization effect. Thus, the model tends to find the noisy label and predict the correct transition matrix T . Next, the loss from the clean and noisy labels can differ greatly. The NLF can filter the noisy ones. Furthermore, the clustering can distinguish between clean and noisy pairs. These three techniques can help the estimated transition matrix converge to the real one.

4.3 Label Probabilistic Modeling and Updating

After we have estimated the transition matrix T , we apply the forward correction to the output from the linear layer $f(\mathbf{x})$ by multiplying T to $f(\mathbf{x})$ as $Tf(\mathbf{x})$. T plays the role of re-weighting $f(\mathbf{x})$, making the model give different confidentiality to the clean

label and noisy label and also adapt to the noise. The optimization goal is to optimize classifier f that minimizes Eq. 4.

5 EXPERIMENT

5.1 Experimental Setting

We implement our approach with PyTorch [24] 1.8.0 and Torchvision 0.9.0 with 2 NVIDIA 2080Ti GPUs. The models are trained using Adam optimizer [14] by setting coefficients of Adam $\beta_1 = 0.9$, $\beta_2 = 0.999$, and $\epsilon = 10^{-8}$. The learning rate is 0.0001 and remains constant during the whole training process. The batch size and total epochs are set to 64 and 50, respectively. In addition, we set the warmup step $\tau = 10$ as the default value.

5.2 Dataset

ISIC Skin Dataset: The ISIC skin dataset [2] comes from the Melanoma Project initiated by the International Skin Imaging Collaboration. There are 2600 melanoma dermoscopy images in this dataset, classifying malignant and benign classes. The dataset consists of 2000 melanoma dermoscopy images for training and 600 for testing. In addition to these data, we also utilize an extra 1582 images from the ISIC training archives for training. All images are resized to 224×224 , and are augmented by randomly adopting horizontal flipping, vertical flipping, or image rotation.

Kaggle Histopathologic Cancer Detection Dataset: The Kaggle histopathologic cancer detection dataset (HCDD) is a marginally modified version of the PatchCamelyon (PCam) [1, 32]. The dataset is a binary classification for malignant and benign, containing low-resolution images of lymph node sections with about 30,000 markers extracted from digital histopathological scans. We randomly select 6200 and 800 images from the training images as our training data and test data, respectively. All the images are resized to the size of 224×224 .

NIH Chest X-Ray Dataset: Wang et al. [33] contains 112,120 frontal-view CXR images from 32,717 patients. Each image is labeled with 14 possible pathological findings that are automatically mined from the text reports. As clean testing data, we employed 1,962 manually labeled images [20]. We resized all the skin images to the size of 224×224 and normalized each image by subtracting ImageNet mean and std.

5.3 Comparison of Classification Results With State-of-the-Art Methods

The performance of our method under different unsupervised loss weights on the histopathologic datasets. To demonstrate the effectiveness of our algorithm, we compare **Pseudo-T correction** with five state-of-the-art noisy label learning methods, including:

(1)**MentorNet (2018)** [11]. MentorNet proposes a neural network to supervise the training of the base deep networks. They used a group of clean data to weigh each training data. This method learns a data-driven curriculum dynamically with the network.

(2)**Co-teaching (2018)** [8]. This method trains two deep neural networks to teach each other given every mini-batch by selecting some data of possibly clean labels. Secondly, the two networks communicate with each other about what data should be used for

Table 1: Comparison of classification results with state-of-the-art methods on ISIC dataset (Accuracy, %). Noise here refers to the noisy sample ratio in the whole dataset. The results are presented in Mean(std) format. The bold numbers are the best result among all the methods.

Dataset	Noise	Cross entropy	Mentornet	Co-teaching	ELR	RMIC	Ours
ISIC	0.05	84.25(0.66)	83.47(0.27)	83.98(0.45)	84.28(0.23)	85.40(0.22)	87.79(0.55)
	0.1	83.01(0.37)	83.83(0.37)	83.39(0.50)	83.18(0.35)	84.33(0.31)	86.39(0.38)
	0.2	81.36(0.61)	82.15(0.49)	83.22(0.21)	83.37(0.48)	84.17(0.32)	85.39(0.26)
	0.4	69.65(0.65)	70.40(0.33)	74.78(0.44)	72.98(0.26)	76.67(0.14)	79.17(0.58)

Table 2: Comparison of classification results with state-of-the-art methods on HCDD dataset(Accuracy, %).

Dataset	Noise	Cross entropy	Mentornet	Co-teaching	ELR	RMIC	Ours
HCDD	0.05	91.28(0.57)	92.65(0.32)	92.88(0.36)	92.69(0.33)	93.88(0.35)	94.11(0.27)
	0.1	88.95(0.31)	91.05(0.27)	91.39(0.48)	90.84(0.24)	92.75(0.30)	92.63(0.36)
	0.2	82.67(0.49)	85.66(0.27)	86.05(0.17)	87.12(0.28)	90.88(0.20)	91.83(0.38)
	0.4	63.41(0.63)	69.43(0.47)	76.03(0.18)	73.86(0.17)	79.00(0.34)	80.48(0.26)

Table 3: The accuracy of different methods on NIH chest X-ray datasets. The average accuracy and standard deviation of 5 random runs are reported and the best results are in bold. The results are presented in Mean(std) format.

Method	Pneumothorax	Nodule or Mass
Cross entropy	0.870(0.33)	0.843(0.39)
Mentornet	0.866(0.27)	0.837(0.31)
Co-teaching	0.873(0.21)	0.820(0.15)
ELR	0.871(0.23)	0.832(0.21)
RMIC	0.891(0.14)	0.846(0.22)
Ours	0.895(0.21)	0.851(0.14)

training. Then, each network updates itself and back-propagates the data chosen by its partner networks.

(3)**ELR (2020)** [19]. A semi-supervised learning technique to generate large probabilities based on the model outputs. Then, ELR develops a regularization term that indirectly prevents memorizing the erroneous labels by guiding the model towards these targets.

(4)**RMIC (2022)** [37]. A collaborative training paradigm with global and local representation learning. They use a self-ensemble model with a noisy label filter to select the clean and noisy samples. Then, the clean samples are trained and applied to eliminate the disturbance from imperfect labeled samples. This method uses a teacher-student co-training strategy for local and global knowledge distillation.

5.3.1 Results on ISIC Dataset. Since the data is more imbalanced and higher proportion of hard samples than the lymph node classification task, it should be noted that the skin lesion classification data is more challenging to use. In the malignant vs. benign classification task on the ISIC dataset, **Pseudo-T correction** significantly outperformed the alternative methods. From Table 1, it is observed that when there is a 0.05 noise ratio setting, the poor sample utilization rate and incorrect hard sample identification in the mild scenario make co-teaching ineffective, while the biased sample selection and down-weighted hard samples in the self-paced Mentornet model

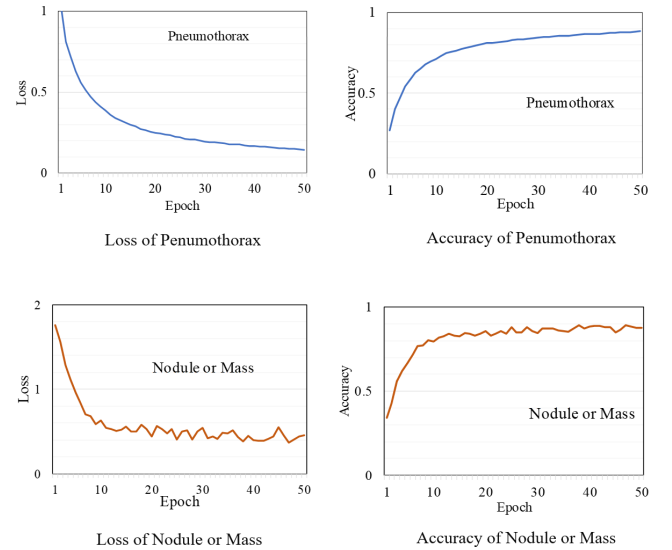


Figure 3: The performance of Pneumothorax and Nodule or Mass on NIH chest X-ray dataset. The first row represents the loss and accuracy of Pneumothorax while the second row represents the loss and accuracy of Nodule or Mass.

hindered its effectiveness. The RMIC discovered a slight increase in accuracy when the noise ratio was low, but when the noise ratio approached 0.4, the performance drastically declined because their cross-entropy loss on small loss data is not reliable in this situation. Compared with our methods, the RMIC led to a minimal difference in accuracy between decentralized training and the baseline, using a noisy dataset led to a much larger difference between the two. The results show that our method can successfully handle noisy labels since the transition matrix can effectively utilize the hard samples and the noise label filter can filter out the noise labels.

5.3.2 Results on HCDD Dataset. To evaluate the generalization ability, Table 2 presents the testing accuracy (summarized from

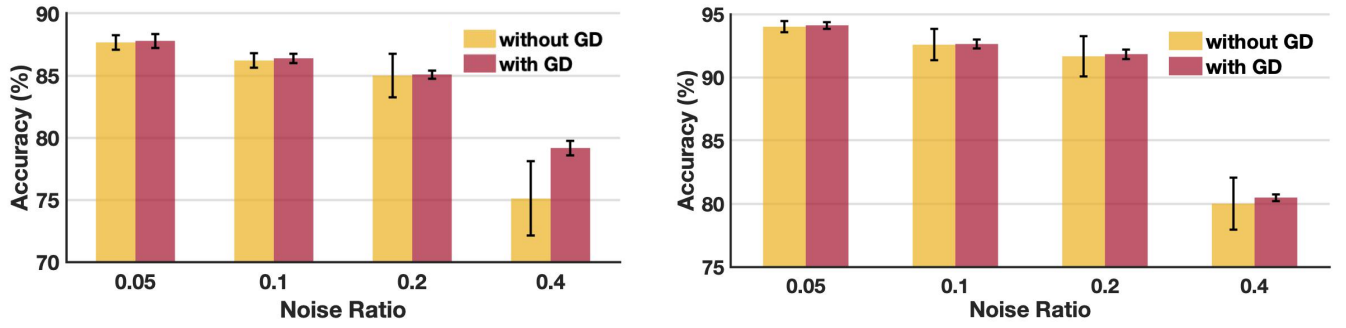
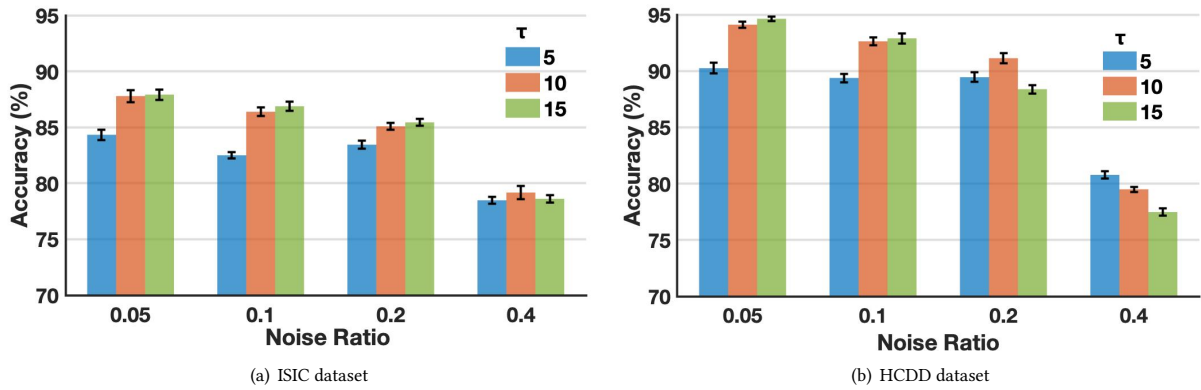


Figure 4: Ablation study on stopping criteria (GD). Left: ISIC, Right: HCDD.

Figure 5: The performance of ablation study under different warmup epochs (τ) and noise ratio on ISIC dataset and HCDD dataset. We report the testing accuracy under distinct settings with the format of mean and std.

three independent runs) of **Pseudo-T correction** and comparison methods on different noise levels. Although the RMIC method achieves the best, 92.75% value at noise equals 0.1 on the HCDD dataset, this method is based on a co-training strategy, so it may be challenging to employ their cross-entropy loss on small loss data. This plausibly implies that **Pseudo-T correction** would be very helpful and practical in clinical applications by fully using the information of noise data.

In addition to successfully handling label noise, our **Pseudo-T correction** is lightweight and easy to implement on resource-limited devices. While using ResNet18 as our base model, **Pseudo-T correction** contains 11.2 million trainable parameters, which is only 1/4 that of RMIC and Co-teaching and around half of the other methods. Compared to RMIC [37], **Pseudo-T correction** gains comparable results to RMIC while being simple and provable.

5.3.3 Results on NIH Chest X-Ray Dataset. NIH is a real-world scenario. We present the comparison in test accuracy with state-of-the-art methods on the NIH chest X-ray dataset in Table 3. From this Table 3, we can observe that **Pseudo-T correction** still outperformed the baseline (e.g., Cross entropy and Co-teaching) and other methods. For instance, **Pseudo-T correction** achieves 2.4% accuracy gains over ELR. Compared to RMIC, our method achieves better performance with 0.5% accuracy-score gains. We explain this

to be that the sample selection is difficult because of the tiny noise proportion and unbalanced sample distribution of the 14 diseases. Overall, this experiment shows the robustness of our method in a real clinical context. Thus, **Pseudo-T correction** is practical with considerably better adaptability.

Furthermore, we reported the loss and accuracy score in Fig. 3. As can be seen from Fig. 3, our method consistently shows good results, showing that the **Pseudo-T correction** can handle the real-world noise. Our method is stable with the high accuracy values. Consequently, it is notable that we present the results on NIH chest X-ray datasets with REAL noise, and the results verify that our method performs well on real noisy datasets.

5.4 Ablation Study

5.4.1 Sanity Check on the Estimated Transition Matrix T . The transition matrix T is an essential element in improving the classification performance. We conducted multiple experiments to prove the correctness of the transition matrix. For sanity check, we visualize the convergence of transition matrix T on the ISIC dataset when the noisy ratio is 0.05 and 0.1. The investigations of T are presented in Table 4. As shown in Table 4, **Pseudo-T correction** achieves ACC of 0.1 noisy ratio gains over 0.35% compared to the without **Pseudo-T correction**. In addition, compared to the without transition matrix correction under a 0.4 noisy ratio, **Pseudo-T**

Table 4: Classification results of with vs. without Pseudo-T correction on ISIC dataset (Accuracy, %). Noise here refers to the noisy sample ratio in the whole dataset. The results are presented in Mean(std) format.

Pseudo-T correction	Noise	ACC (std)	Pseudo-T correction	Noise	ACC (std)
w	0	88.74 (1.23)	w/o	0	87.73 (1.10)
	0.05	87.64 (0.12)		0.05	87.53 (1.03)
	0.1	86.88 (1.12)		0.1	86.53 (1.24)
	0.2	84.66 (0.96)		0.2	84.53 (1.61)
	0.4	81.11 (1.67)		0.4	76.41 (2.62)

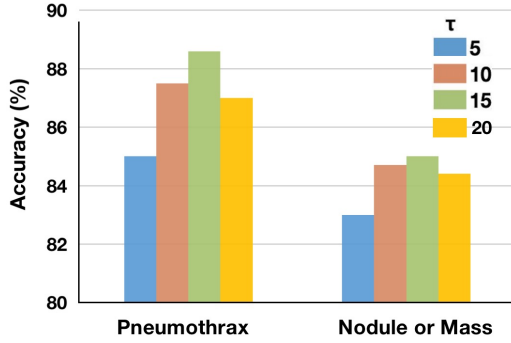


Figure 6: The performance of ablation study under different warmup epochs (τ) and noise ratio on NIH chest X-ray dataset. We report the testing accuracy under distinct settings.

correction added after it achieves significant performance improvement, especially with the increase of 4.7% ACC. Experimental results indicate that the minimization of the corrected loss under the noise distribution corrected by the correction matrix is the same as the minimization of the original loss under the true label distribution. It demonstrates the advantages of using **Pseudo-T correction** to reduce the risk of training a classification model with incorrect information because the chances of randomly selecting a complementing label that is not a real label are high.

5.4.2 Influence of Stopping Criteria (GD). To evaluate the stopping criteria (GD) on the ISIC dataset and the HCDD dataset, we report the results in Fig. 4. It can be seen from Fig. 4 that the proposed **Pseudo-T correction** produces overall good results under a distinct noise ratio. As shown in Fig. 4, we report the comparison results with vs. without stopping criteria (GD). From Fig. 4, the “with GD” achieves the improvement of 4.07% compared with “without GD” under 0.4 noise rate on the ISIC dataset. Equally, under the noise rate is 0.05, our method achieves a good result with GD. At a noise rate of 0.4, “with GD” increases the accuracy over “without GD” by 1.3% on the HCDD dataset. Fig. 4 suggests that our method using stopping criteria produces the overall better performance, compared with that without stopping criteria on ISIC and HCDD datasets. This means that our method would be very helpful in noisy data by using gradient disparity as an effective criterion to avoid overfitting noisy data with iterative methods.

5.4.3 Influence of Warmup Epoch. We evaluate the influence of warmup epoch, by comparing the results of **Pseudo-T correction** using different pre-training epochs under the settings of different

noise ratios. Specifically, we vary the noise ratio from the range of [0.05, 0.1, 0.2, 0.4] and record the results in Fig. 5. It can be seen from Fig. 5(a) that, with a very low warmup epoch (e.g., $\tau = 5$), our method cannot yield good results. With $\tau = 10$, we can obtain relatively better results. The results are reported in Fig. 5(a), **Pseudo-T correction** using 0.05 noisy ratio and 15 warmup epochs to produce the best performance on the ISIC dataset. The main reason could be that the warmup epoch helps extract robust features of noisy samples.

Similarly, it can be seen from Fig. 5(b) that **Pseudo-T correction** yields consistently better results within the range of [0.05, 0.1], when τ is equal to 15. This Fig. 5(b) also shows that, with $\tau = 10$, **Pseudo-T correction** achieves the overall best performances under a noise ratio of 0.2. Also, these results imply that the warmup epoch is an important parameter for maintaining model stability.

We further analyze how the warmup epoch τ on NIH chest X-ray dataset. We ranged $\tau \in [5, 10, 15, 20]$. As shown in Fig. 6, we can observe that the best selection of τ is set to 15. From 5 to 15, increasing τ can improve the classification performance. The performance slightly drops when τ is set to 20. Thus, we report the performance of the proposed method by setting τ to 20 on NIH chest X-ray dataset, unless otherwise specified. We find that increasing the τ may not always improve the performance yet brings extra computational cost. It also demonstrates that increasing τ is not always the best choice for architectural design.

6 CONCLUSION

In this work, we present a simple and provable method by utilizing noisy labels for medical image analysis. The proposed method (**Pseudo-T correction**) does not rely on relabeling the noisy labeled data and directly uses noisy labeled data and a lightweight network to promote the learning of robust representation features. Notably, to tackle the realistic but ignored issue of incomplete information in noisy labels, we designed a transition matrix, that corrects model predictions. Furthermore, to avoid underfitting or overfitting deep neural networks trained with iterative methods, resulting in inaccurate transition matrix estimation. Therefore, we employ gradient disparity as a criterion to decide if fixing the transition matrix in the further model training steps. Extensive experiments on three challenging medical datasets, including dermoscopic images, histopathology slide images, X-Ray, about medical image classification tasks with random noise and inter-observer variability, demonstrate that our method obtains state-of-the-art performance. In the future, we will fuse multi-class classification tasks to address the data heterogeneity issue and apply our methods to further improve performance on more datasets.

REFERENCES

- [1] Babak Ehteshami Bejnordi, Mitko Veta, Paul Johannes Van Diest, Bram Van Ginneken, Nico Karssemeijer, Geert Litjens, Jeroen AWM Van Der Laak, Meyke Hermesen, Quirine F Manson, Maschenka Balkenhol, et al. 2017. Diagnostic assessment of deep learning algorithms for detection of lymph node metastases in women with breast cancer. *Jama* 318, 22 (2017), 2199–2210.
- [2] Noel CF Codella, David Gutman, M Emre Celebi, Brian Helba, Michael A Marchetti, Stephen W Dusza, Aadi Kallou, Konstantinos Liopyris, Nabin Mishra, Harald Kittler, et al. 2018. Skin lesion analysis toward melanoma detection: A challenge at the 2017 international symposium on biomedical imaging (isbi), hosted by the international skin imaging collaboration (isic). In *2018 IEEE 15th international symposium on biomedical imaging (ISBI 2018)*. IEEE, 168–172.
- [3] Jeffrey De Fauw, Joseph R Ledsam, Bernardino Romera-Paredes, Stanislav Nikolov, Nenad Tomasev, Sam Blackwell, Harry Askham, Xavier Glorot, Brendan O'Donoghue, Daniel Visentin, et al. 2018. Clinically applicable deep learning for diagnosis and referral in retinal disease. *Nature medicine* 24, 9 (2018), 1342–1350.
- [4] Yair Dgani, Hayit Greenspan, and Jacob Goldberger. 2018. Training a neural network based on unreliable human annotation of medical images. In *2018 IEEE 15th International Symposium on Biomedical Imaging (ISBI 2018)*. 39–42. <https://doi.org/10.1109/ISBI.2018.8363518>
- [5] Jared A Dunnmon, Alexander J Ratner, Khaled Saab, Nishith Khandwala, Matthew Markert, Hersh Sagreiya, Roger Goldman, Christopher Lee-Messer, Matthew P Lungren, Daniel L Rubin, et al. 2020. Cross-modal data programming enables rapid medical machine learning. *Patterns* 1, 2 (2020).
- [6] Andre Esteva, Brett Kuprel, Roberto A Novoa, Justin Ko, Susan M Swetter, Helen M Blau, and Sebastian Thrun. 2017. Dermatologist-level classification of skin cancer with deep neural networks. *nature* 542, 7639 (2017), 115–118.
- [7] Alba García Seco de Herrera, Antonio Foncubierta-Rodríguez, Dimitrios Markonis, Roger Schaer, and Henning Müller. 2014. Crowdsourcing for medical image classification. *Swiss Medical Informatics* (2014).
- [8] Bo Han, Quanming Yao, Xingrui Yu, Gang Niu, Miao Xu, Weihua Hu, Ivor Tsang, and Masashi Sugiyama. 2018. Co-teaching: Robust training of deep neural networks with extremely noisy labels. *Advances in neural information processing systems* 31 (2018).
- [9] Kaiming He, Xiangyu Zhang, Shaoqing Ren, and Jian Sun. 2016. Deep residual learning for image recognition. In *Proceedings of the IEEE conference on computer vision and pattern recognition*. 770–778.
- [10] Ahmet Iscen, Jack Valmadre, Anurag Arnab, and Cordelia Schmid. 2022. Learning with Neighbor Consistency for Noisy Labels. [arXiv:2202.02200](https://arxiv.org/abs/2202.02200) [cs.CV]
- [11] Lu Jiang, Zhengyuan Zhou, Thomas Leung, Li-Jia Li, and Li Fei-Fei. 2018. MentorNet: Learning Data-Driven Curriculum for Very Deep Neural Networks on Corrupted Labels. [arXiv:1712.05055](https://arxiv.org/abs/1712.05055) [cs.CV]
- [12] Taehyeon Kim, Jongwoo Ko, JinHwan Choi, Se-Young Yun, et al. 2021. FINE Samples for Learning with Noisy Labels. *Advances in Neural Information Processing Systems* 34 (2021).
- [13] Youngdong Kim, Junho Yim, Juseung Yun, and Junmo Kim. 2019. NLNL: Negative Learning for Noisy Labels. [arXiv:1908.07387](https://arxiv.org/abs/1908.07387) [cs.LG]
- [14] Diederik P Kingma and Jimmy Ba. 2014. Adam: A method for stochastic optimization. [arXiv preprint arXiv:1412.6980](https://arxiv.org/abs/1412.6980) (2014).
- [15] Mingwei Leng, Haitao Tang, and Xiaoyun Chen. 2007. An Efficient K-means Clustering Algorithm Based on Influence Factors. In *Eighth ACIS International Conference on Software Engineering, Artificial Intelligence, Networking, and Parallel/Distributed Computing (SNPD 2007)*, Vol. 2. 815–820. <https://doi.org/10.1109/SNPD.2007.279>
- [16] Jingling Li, Mozhi Zhang, Keyulu Xu, John Dickerson, and Jimmy Ba. 2021. How does a Neural Network's Architecture Impact its Robustness to Noisy Labels? *Advances in Neural Information Processing Systems* 34 (2021).
- [17] Jiarun Liu, Ruirui Li, and Chuan Sun. 2021. Co-correcting: noise-tolerant medical image classification via mutual label correction. *IEEE Transactions on Medical Imaging* 40, 12 (2021), 3580–3592.
- [18] Luyan Liu, Zhengdong Zhang, Shuai Li, Kai Ma, and Yefeng Zheng. 2021. S-CUDA: Self-cleansing unsupervised domain adaptation for medical image segmentation. *Medical Image Analysis* 74 (2021), 102214.
- [19] Sheng Liu, Jonathan Niles-Weed, Narges Razavian, and Carlos Fernandez-Granda. 2020. Early-learning regularization prevents memorization of noisy labels. *Advances in neural information processing systems* 33 (2020), 20331–20342.
- [20] Anna Majkowska, Sid Mittal, David F Steiner, Joshua J Reicher, Scott Mayer McKinney, Gavin E Duggan, Krish Eswaran, Po-Hsuan Cameron Chen, Yun Liu, Sreenivasa Raju Kalidindi, et al. 2020. Chest radiograph interpretation with deep learning models: assessment with radiologist-adjudicated reference standards and population-adjusted evaluation. *Radiology* 294, 2 (2020), 421–431.
- [21] Riccardo Miotto, Fei Wang, Shuang Wang, Xiaoqian Jiang, and Joel T Dudley. 2018. Deep learning for healthcare: review, opportunities and challenges. *Briefings in bioinformatics* 19, 6 (2018), 1236–1246.
- [22] D. Napoleon and P. Ganga Lakshmi. 2010. An efficient K-Means clustering algorithm for reducing time complexity using uniform distribution data points. In *Trendz in Information Sciences & Computing (TISC2010)*. 42–45. <https://doi.org/10.1109/TISC.2010.5714605>
- [23] Sébastien Ourselin, Radu Stefanescu, and Xavier Pennec. 2002. Robust registration of multi-modal images: towards real-time clinical applications. In *International Conference on Medical Image Computing and Computer-Assisted Intervention*. Springer, 140–147.
- [24] Adam Paszke, Sam Gross, Soumith Chintala, Gregory Chanan, Edward Yang, Zachary DeVito, Zeming Lin, Alban Desmaison, Luca Antiga, and Adam Lerer. 2017. Automatic differentiation in pytorch. (2017).
- [25] Giorgio Patrini, Alessandro Rozza, Aditya Krishna Menon, Richard Nock, and Lizhen Qu. 2017. Making deep neural networks robust to label noise: A loss correction approach. In *Proceedings of the IEEE conference on computer vision and pattern recognition*. 1944–1952.
- [26] Azhar Rauf, Saeed Mahfooz Sheeba, Shah Khuroo, Huma Javed, et al. 2012. Enhanced k-mean clustering algorithm to reduce number of iterations and time complexity. *Middle-East Journal of Scientific Research* 12, 7 (2012), 959–963.
- [27] Scott Reed, Honglak Lee, Dragomir Anguelov, Christian Szegedy, Dumitru Erhan, and Andrew Rabinovich. 2015. Training Deep Neural Networks on Noisy Labels with Bootstrapping. [arXiv:1412.6596](https://arxiv.org/abs/1412.6596) [cs.CV]
- [28] Arnaud Arindra Adiyoso Setio, Alberto Traverso, Thomas De Bel, Moira SN Berens, Cas Van Den Bogaard, Piergiorgio Cerello, Hao Chen, Qi Dou, Maria Evelina Fantacci, Bram Geurts, et al. 2017. Validation, comparison, and combination of algorithms for automatic detection of pulmonary nodules in computed tomography images: the LUNA16 challenge. *Medical image analysis* 42 (2017), 1–13.
- [29] John Stoitsis, Ioannis Valavanis, and Stavroula G Mougiakakou. 2006. Computer aided diagnosis based on medical image processing and artificial intelligence methods. *Nuclear Instruments and Methods in Physics Research Section A* 569, 2 (2006), 591–595.
- [30] Sainbayar Sukhbaatar, Joan Bruna, Manohar Paluri, Lubomir Bourdev, and Rob Fergus. 2014. Training convolutional networks with noisy labels. [arXiv:1406.2080](https://arxiv.org/abs/1406.2080) (2014).
- [31] Brendan Van Rooyen and Robert C Williamson. 2017. A Theory of Learning with Corrupted Labels. *J. Mach. Learn. Res.* 18, 1 (2017), 8501–8550.
- [32] Bastiaan S Veeling, Jasper Linmans, Jim Winkens, Taco Cohen, and Max Welling. 2018. Rotation equivariant CNNs for digital pathology. In *International Conference on Medical image computing and computer-assisted intervention*. Springer, 210–218.
- [33] Xiaosong Wang, Yifan Peng, Le Lu, Zhiyong Lu, Mohammadhadi Bagheri, and Ronald M Summers. 2017. Chestx-ray8: Hospital-scale chest x-ray database and benchmarks on weakly-supervised classification and localization of common thorax diseases. In *Proceedings of the IEEE conference on computer vision and pattern recognition*. 2097–2106.
- [34] Xiaosong Wang, Yifan Peng, Le Lu, Zhiyong Lu, and Ronald M Summers. 2018. Tienet: Text-image embedding network for common thorax disease classification and reporting in chest x-rays. In *Proceedings of the IEEE conference on computer vision and pattern recognition*. 9049–9058.
- [35] Cheng Xue, Qiao Deng, Xiaomeng Li, Qi Dou, and Pheng-Ann Heng. 2020. Cascaded robust learning at imperfect labels for chest x-ray segmentation. In *International conference on medical image computing and computer-assisted intervention*. Springer, 579–588.
- [36] Cheng Xue, Qi Dou, Xueying Shi, Hao Chen, and Pheng-Ann Heng. 2019. Robust learning at noisy labeled medical images: Applied to skin lesion classification. In *2019 IEEE 16th International Symposium on Biomedical Imaging (ISBI 2019)*. IEEE, 1280–1283.
- [37] Cheng Xue, Lequan Yu, Pengfei Chen, Qi Dou, and Pheng-Ann Heng. 2022. Robust Medical Image Classification from Noisy Labeled Data with Global and Local Representation Guided Co-training. *IEEE Transactions on Medical Imaging* (2022).
- [38] Samir S Yadav and Shivajirao M Jadhav. 2019. Deep convolutional neural network based medical image classification for disease diagnosis. *Journal of Big Data* 6, 1 (2019), 1–18.
- [39] Haidong Zhu, Jialin Shi, and Ji Wu. 2019. Pick-and-learn: automatic quality evaluation for noisy-labeled image segmentation. In *International Conference on Medical Image Computing and Computer-Assisted Intervention*. Springer, 576–584.